Physical Status of the Intracluster Medium Investigated through Radio and X-ray Observations

Motokazu Takizawa
(Yamagata University)

Itahana, Takizawa et al. (2015), PASJ, 67, 113
Itahana, Takizawa et al. (2017), PASJ, 69, 88
Akahori,,,Machida,,,Takizawa et al. PASJ in press
(arXiv:1709.02072)

Mineshige Group OBOG Workshop
16 December 2017@Kanpo no Yado Arima

A Brief Self-Introduction

- Name: Motokazu Takizawa (滝沢元和)
  - Got PhD in March 1999
  - Posdoc at Rescue, Univ. of Tokyo (1999--2000)
  - Yamagata Univ. (2000--present)
  - Univ. of Virginia (2001-2002)
- (Maybe) the 5-th student after Mineshige-san came to “Ubutsu” (Department of Astronomy, Kyoto Univ.).
- Research intersts
  - Clusters of Galaxies
    - Non-therma Phenomena (high energy particles, magnetic fields, turbulence, etc)
    - Multiwave Observations (X-ray, radio, weak lensing, SZ, etc)
  - Numerical Simulations
    - Hydrodynamics &Magnetohydrodynamics
    - N-body Problems
    - Parallel Computing

Radio Halos / Relics

- Some merging clusters have diffuse non-thermal radio emitting regions.
  ($E_e \sim$GeV, B$\sim\mu$G)
- Radio halos and (mini halos)
  - Located near the center, similar to X-ray morphology
  - Associated with ICM turbulence???
- Radio relics
  - Located in the outskirts, arc-like shape,
  - Likely associated with ICM shocks?

Abell 2319 with Radio Halo
Rosat X-ray image (colors)
Radio image (contours)
Feretti et al. 1997

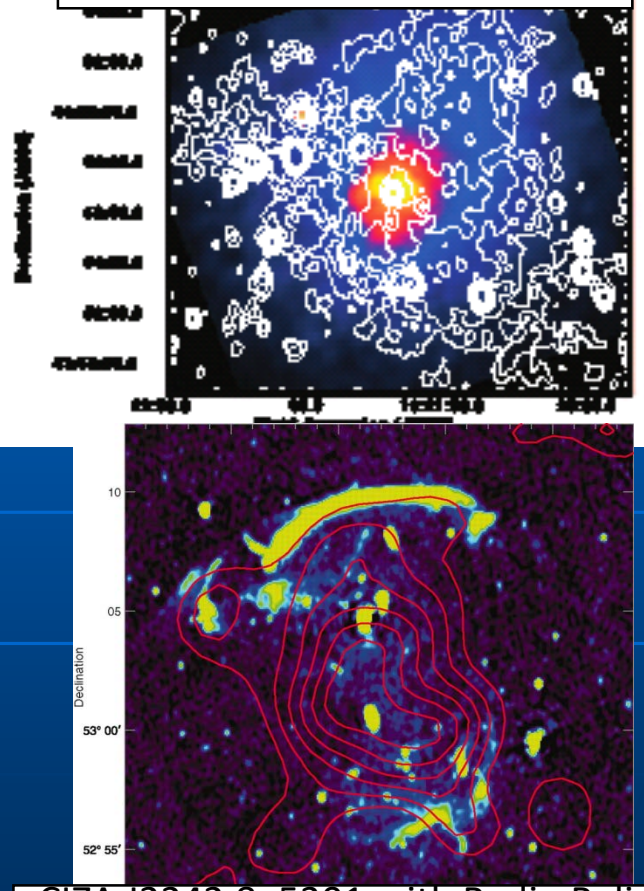

CIZA J2242.8+5301 with Radio Relic
Rosat X-ray image (contours)
Radio image (colors)
Van Weeren et al. 2010

Mach Number Estimation of Shocks at Radio Relics : Two Methods

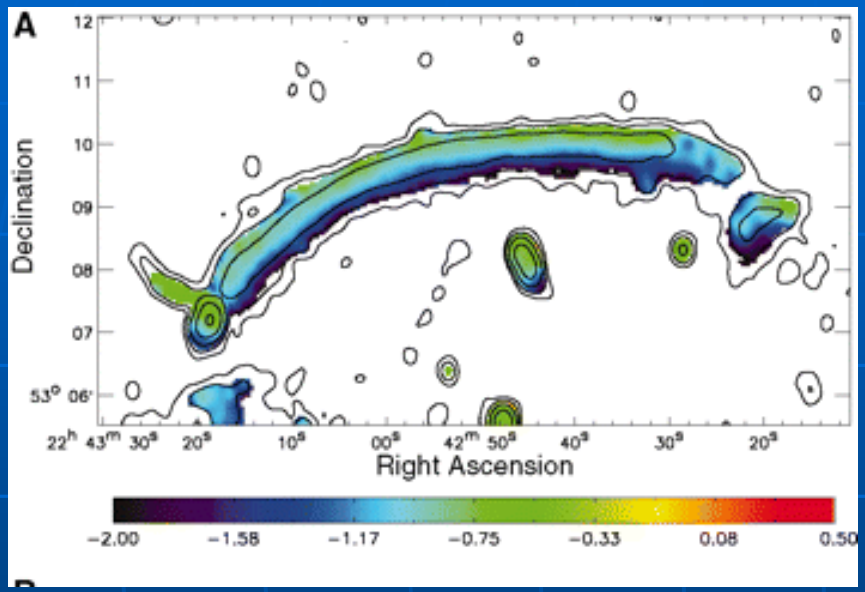

Radio Spectral index map of the relic in CIZA J2242.8+5301 (Van Weeren et al. 2010)

$F_\nu \propto \nu^{-\alpha}$ --> $N(E_e) \propto E_e^{-(2\alpha+1)}$

With a (simple) diffusive shock accerelation model,

--->

$M^2 = (2\alpha+2)/(2\alpha-2)$

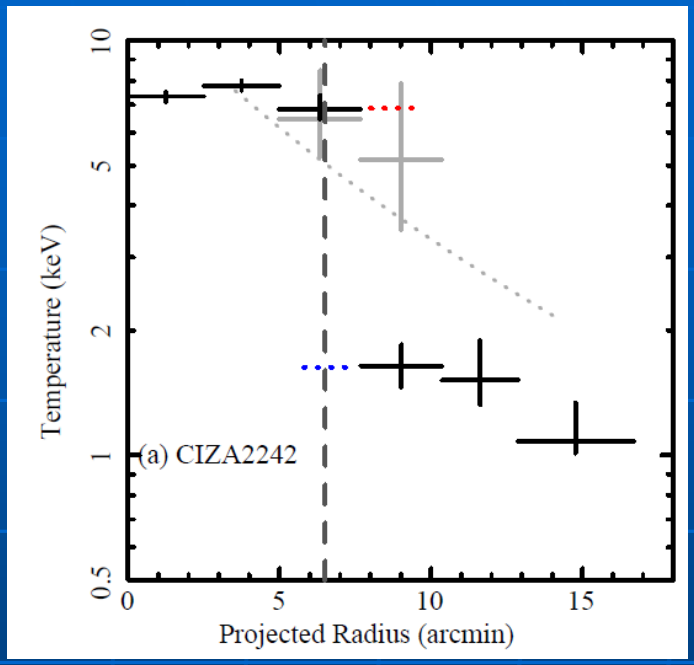

Temperature Profile across the relic in CIZA J2242.8+5301 (Akamatsu & Kawahara 2013)

With the RH relation

---->

$T_{post}/T_{pre} = (5M^4+14M^2-3)/(16M^2)$

Radio Relics: Mach Number consistency???

- Akamatsu&Kawahara (2013) suggests that M_X and M_{radio} seem to be consistent with each other.
- A simple model of diffusive shock acceleration is correct?
- However, sample size is obviously too small to say something definite.

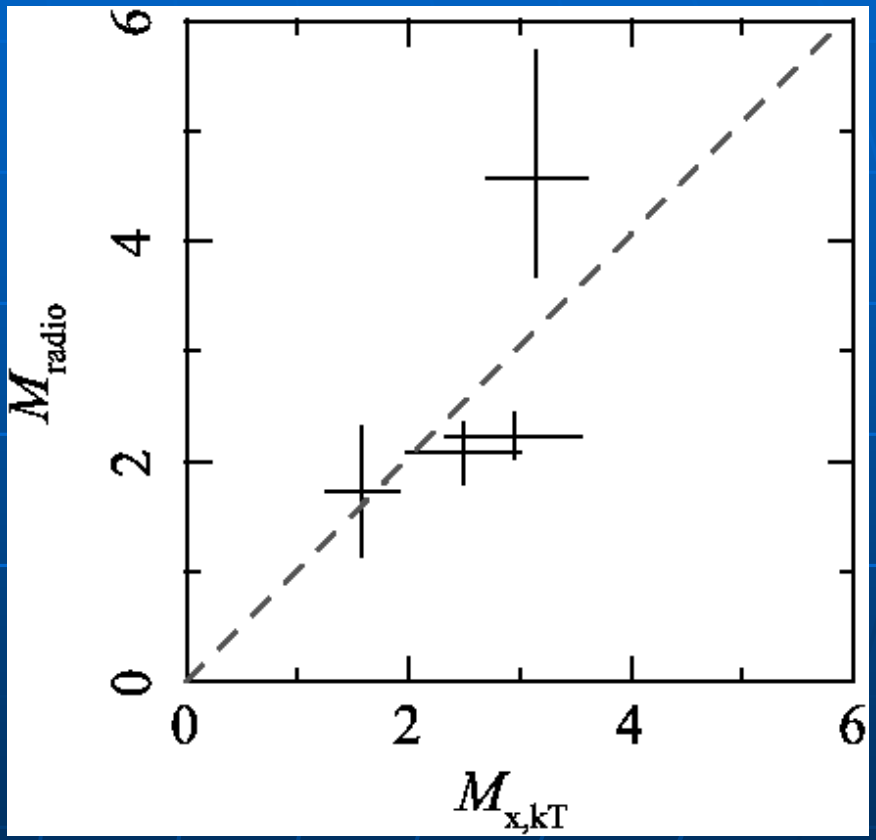

Akamatsu&Kawahara (2013)

1RXS J0603.3+4214 with “toothbrush-relic”

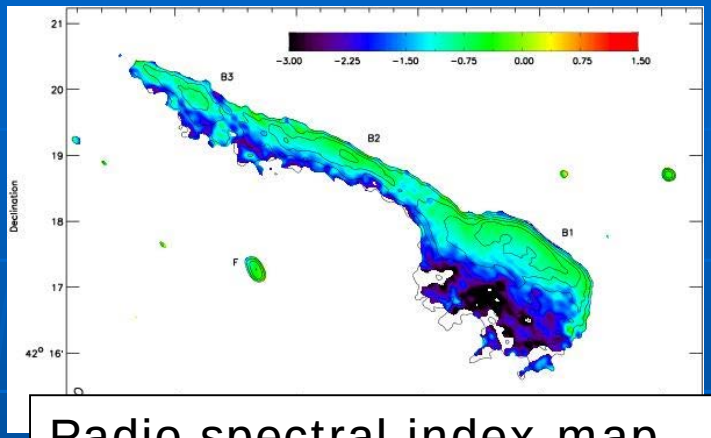

Radio spectral index map (van Weeren et al. 2012)

α_{inj}=0.6−0.7 ---> M_{radio}=3.3−4.6

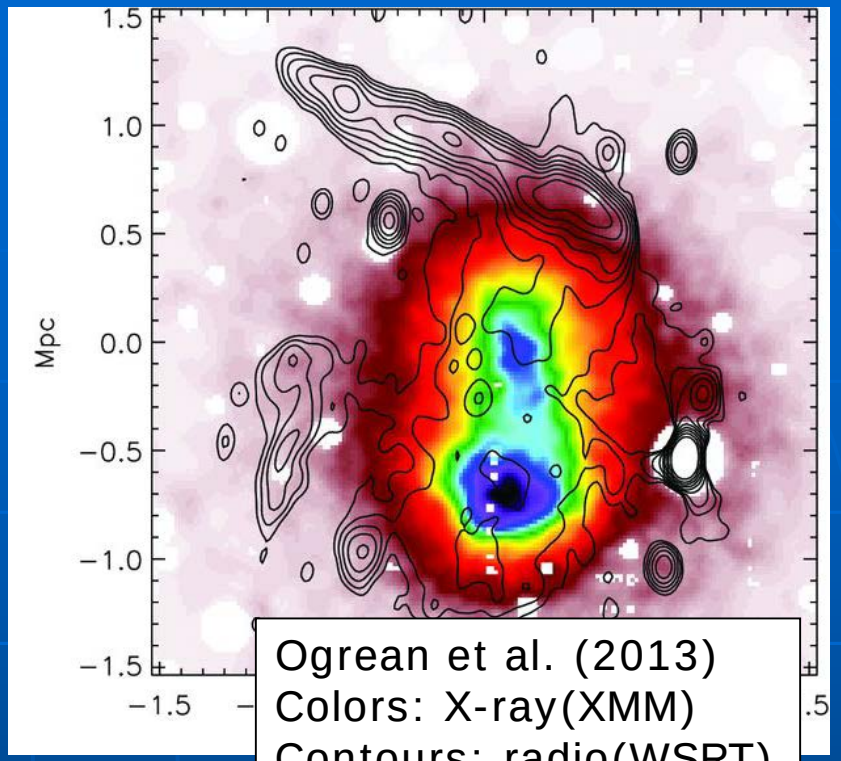

Ogrean et al. (2013)
Colors: X-ray(XMM)
Contours: radio(WSRT)

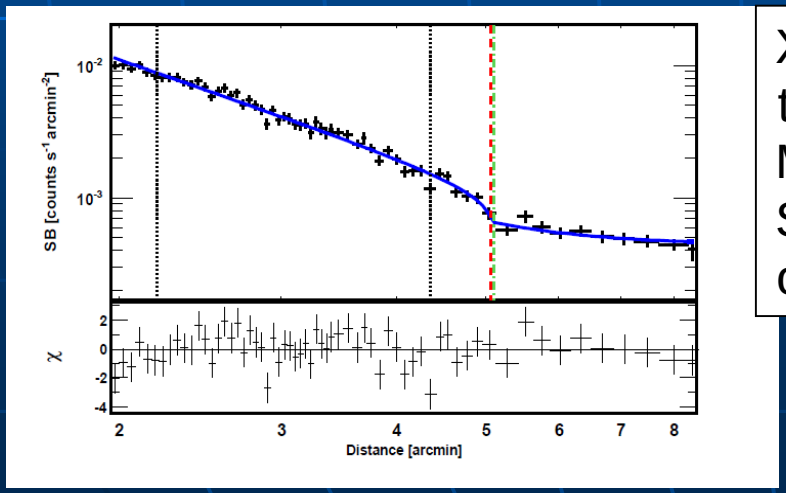

X-ray surface brightness profile across the relic (Ogrean et al. 2013)

$M_X = 1.7^{+0.41}_{-0.42}$

Shock is shifted outward from the relic outer edge????

$$\frac{\rho_2}{\rho_1} = \frac{4M_X^2}{M_X^2 + 3}$$

toothbrush-relic: temperature profile across the relic (Itahana et al. 2015)

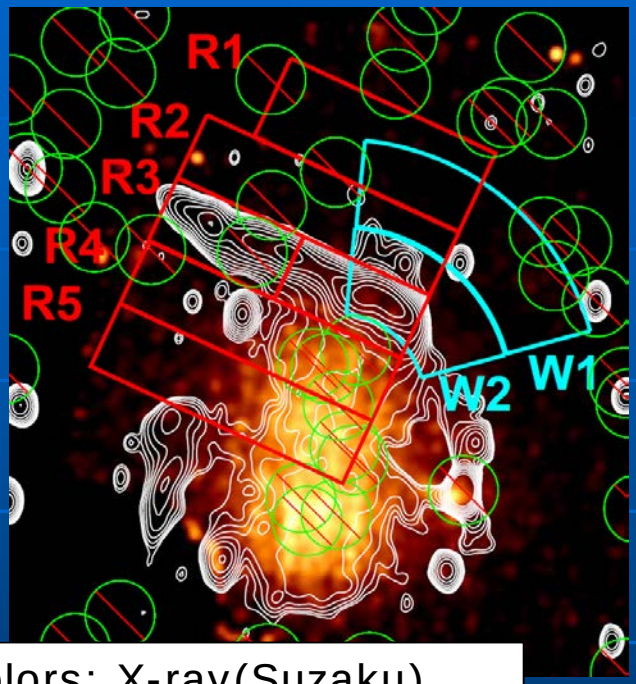

Colors: X-ray(Suzaku)
Contours: radio(WSRT)

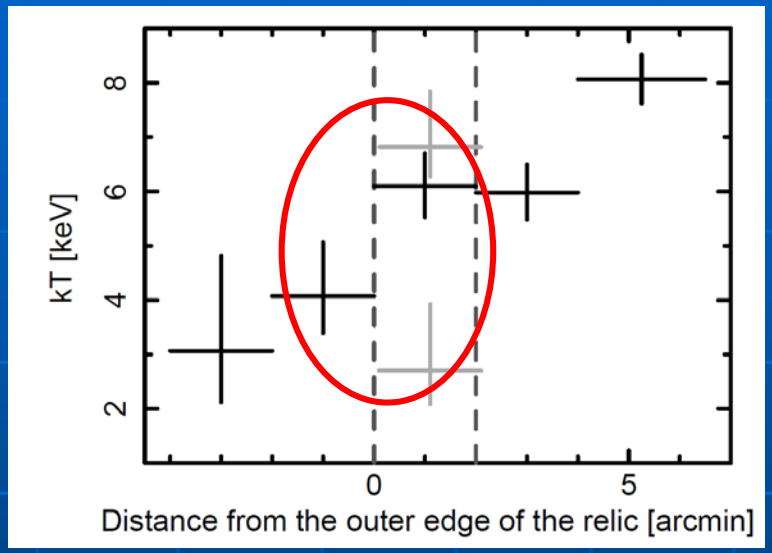

$$\frac{T_2}{T_1} = \frac{5{M_X}^4 + 14{M_X}^2 - 3}{16{M_X}^2}$$

- Obtained Mach number

$$1.50^{+0.37+0.25+0.14}_{-0.27-0.24-0.15}$$

- Similar to the XMM results(Ogrean et al. 2013, surface brightness analysis), but more robust for uncertainties of line-of-sight structures.
- Inconsistent with radio results.

After our work,,,(van Weeren et al. 2016)

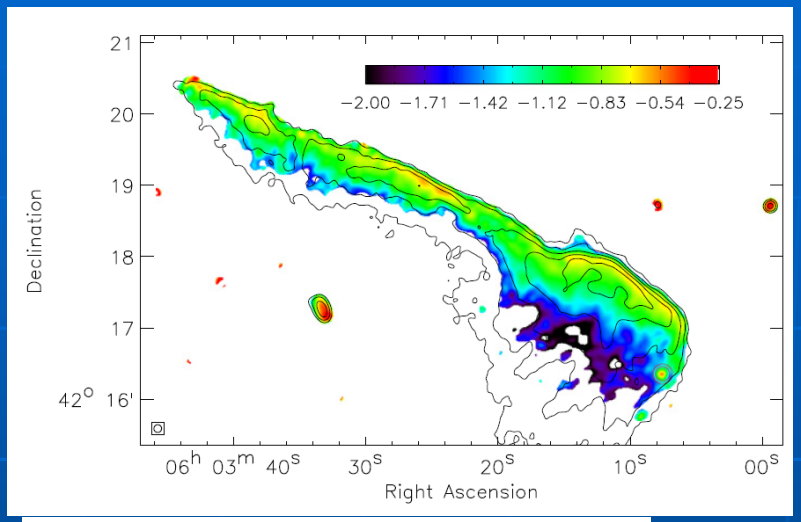

- New radio data (LOFAR+VLA) show steeper spectra.

$$\alpha = -0.8 \pm 0.1$$

$$\mathcal{M} = 2.8^{+0.5}_{-0.3},$$

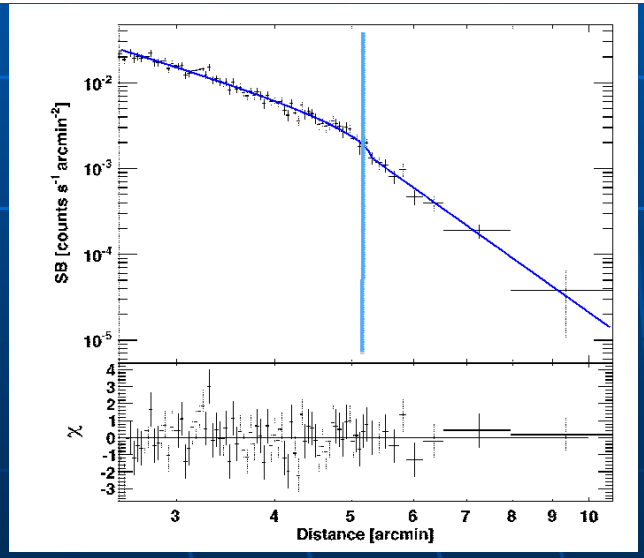

- Chandra X-ray data indicate shock is just at the outer edge of the relic, maybe XMM result is incorrect.

$\mathcal{M} \approx 1.2$, with an upper limit of $\mathcal{M} \approx 1.5$

RXC J1053.7+5453

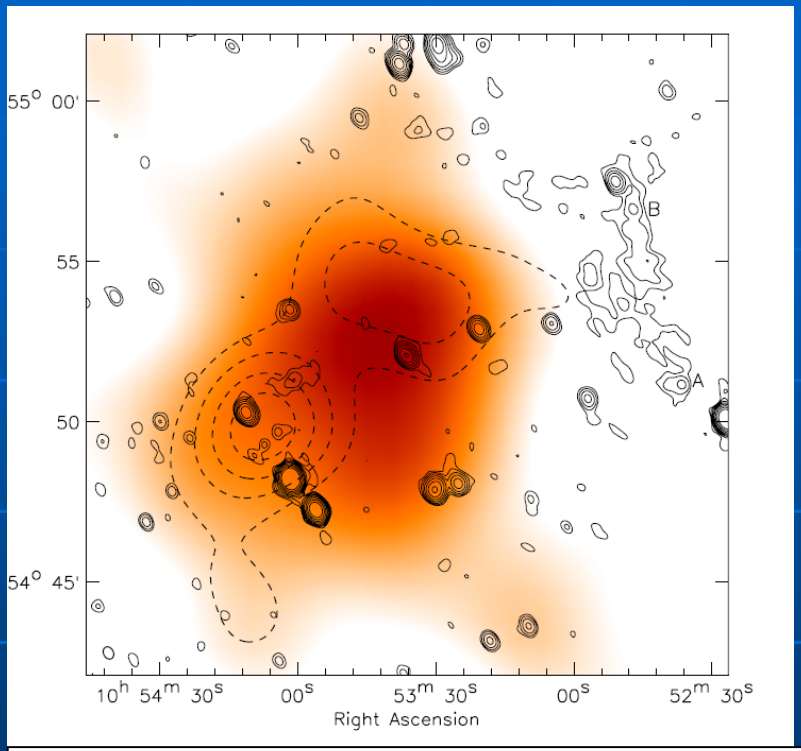

van Weeren (2011)

Colors: X-ray(ROSAT)
Solid contours: radio(WSRT)
Dotted contours: galaxy distribution

- Elongated X-ray morphology, with radio relic (van Weeren et al. 2011)
- Two subgroups in galaxy distribution.
- No direct temperature measurements (kT ~3keV is expected from L_X-kT relation)
- No radio spectrum information

RXC J1053: temperature profile across the relic (Itahana et al. 2017)

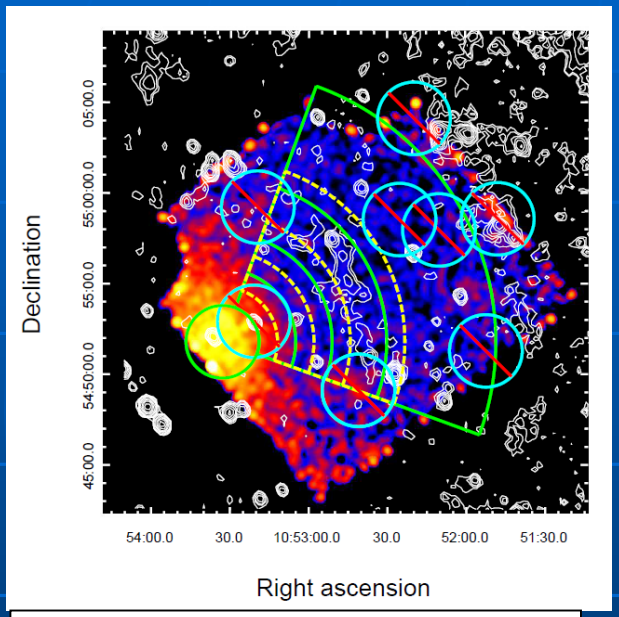

Colors: X-ray(Suzaku)
contours: radio(WSRT)

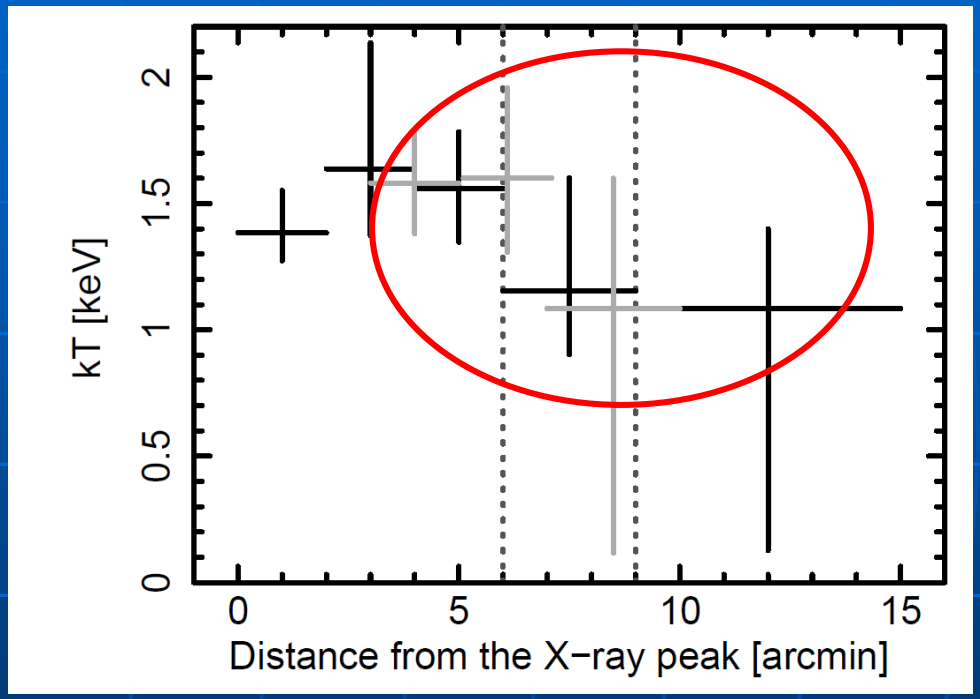

$$\frac{T_2}{T_1} = \frac{5{M_X}^4 + 14{M_X}^2 - 3}{16{M_X}^2}$$

$$M_X = 1.44^{+0.48+0.14+0.03}_{-0.91-1.34-0.04}$$

- Unfortunately, we do not have any radio spectral inormation.

RXC J1053: Surface britness edge (Itahana et al. 2017)

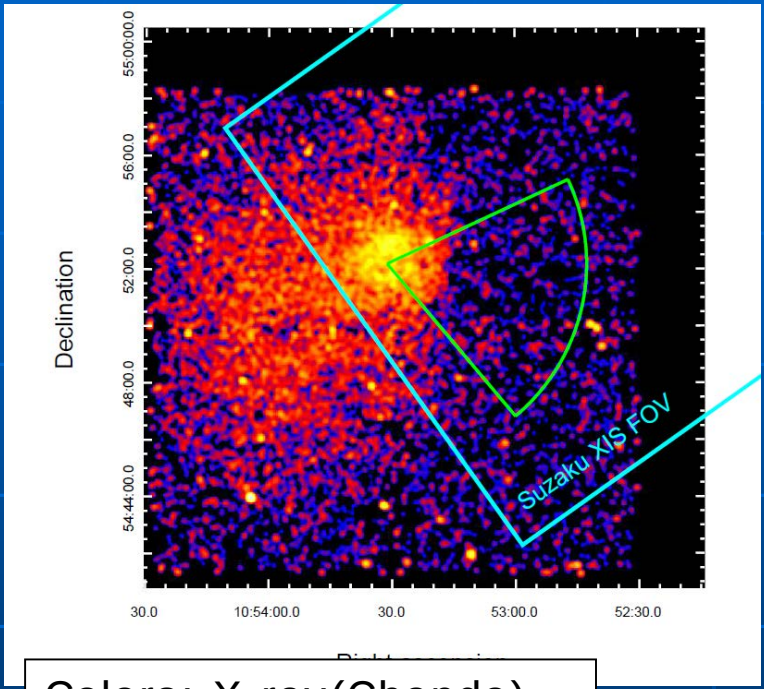

Colors: X-ray(Chanda)

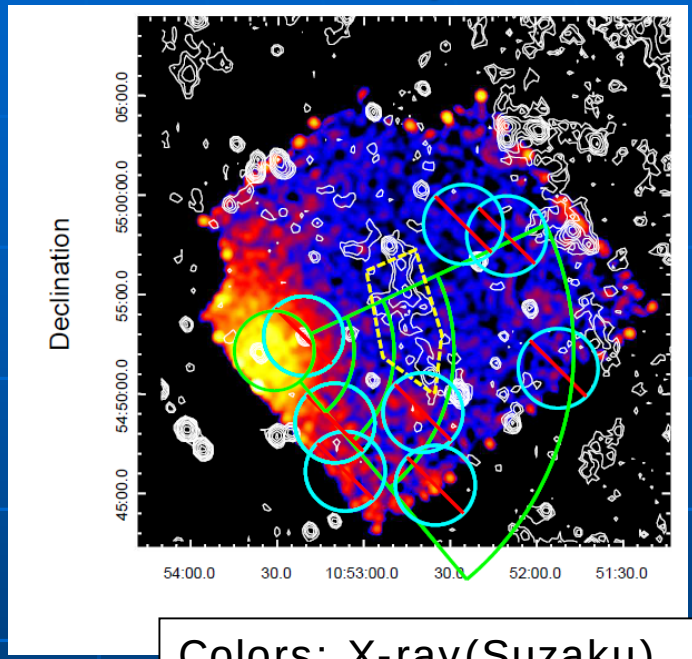

Colors: X-ray(Suzaku)
contours: radio(WSRT)

- We found surface brightness edge, between the cluster X-ray peak and relic.
- This indicates the discontinuity in density structure.
- Shock?, contact discontinuity?, others?

RXC J1053: Surface britness edge (2) (Itahana et al. 2017)

Surface brigtness profile

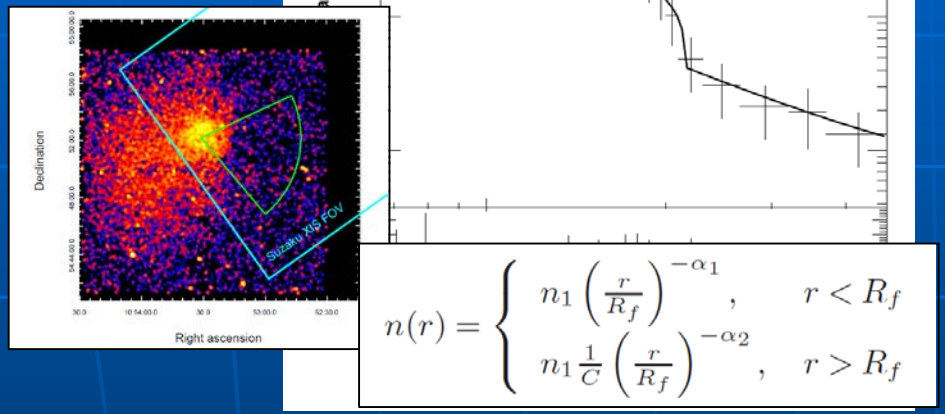

$$n(r) = \begin{cases} n_1 \left(\frac{r}{R_f}\right)^{-\alpha_1}, & r < R_f \\ n_1 \frac{1}{C} \left(\frac{r}{R_f}\right)^{-\alpha_2}, & r > R_f \end{cases}$$

Temperature profile

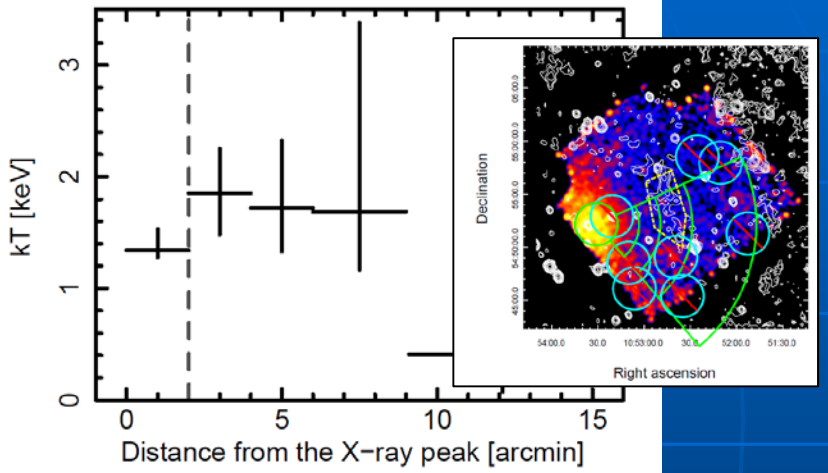

Fig. 8. The temperature profile across the surface brightness edge. The position of the surface brightness edge is displayed by dark gray dotted line.

$$n_1/n_2 = 2.44^{+2.50}_{-1.22}$$

$$T_1/T_2 = 0.72^{+0.24}_{-0.15}$$

$$P_1/P_2 = 1.76^{+1.89}_{-0.95}$$

- This is not a shock, may be a contact discontinuity.

Radio relic Mach number problem: updated version

Akamatsu&Kawahara (2013)

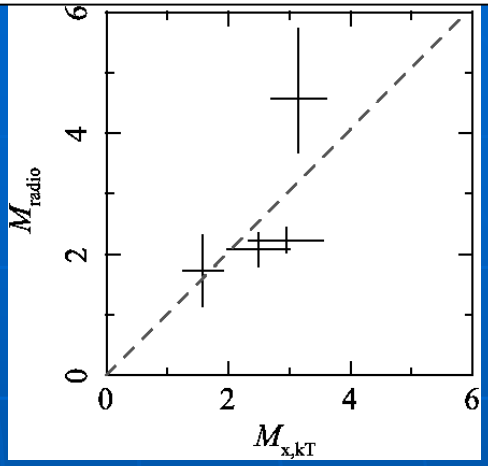

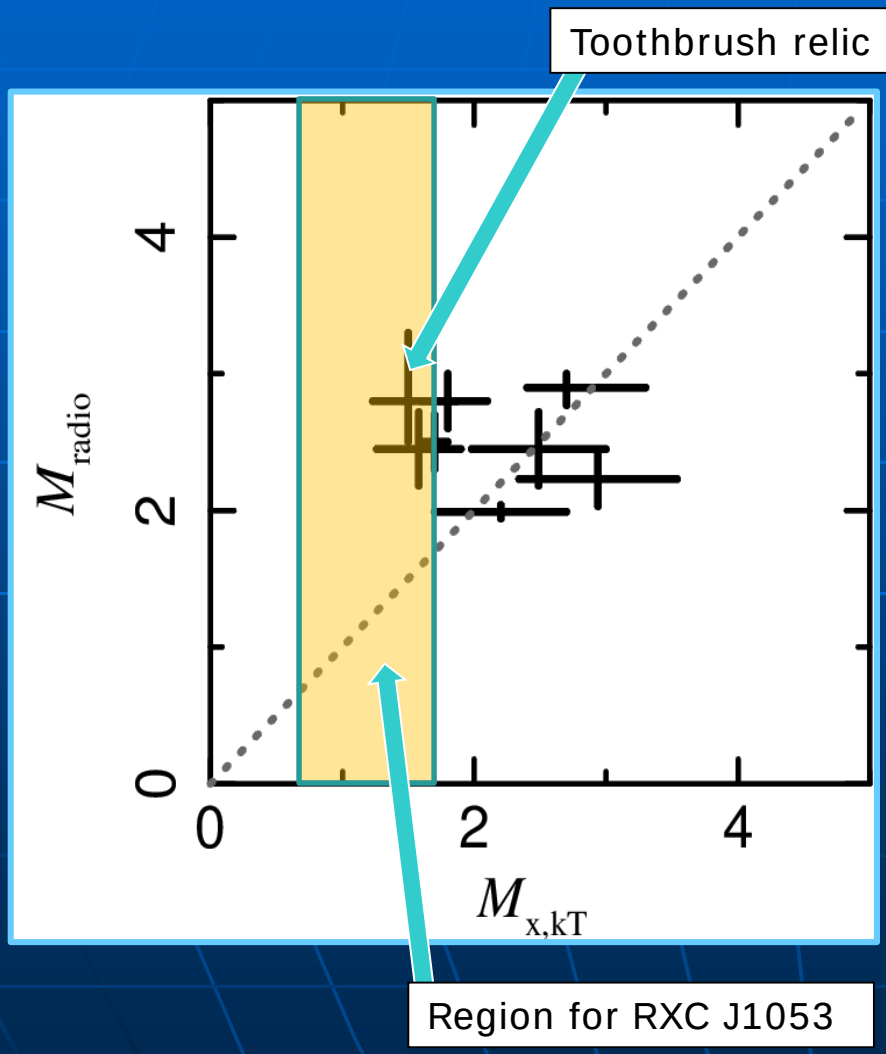

- Sample size becomes slightly larger.
- Some radio results has been changed.
- Basically, M_X and M_{radio} seems to be consisitent with each other, but some outliers like “toothbrush” may exist.

PASJ review paper(arXiv:1709.02072)

Cosmic Magnetism in Centimeter and Meter Wavelength Radio Astronomy

Takuya AKAHORI[1]*, Hiroyuki NAKANISHI[1], Yoshiaki SOFUE[2], Yutaka FUJITA[3], Kiyotomo ICHIKI[4], Shinsuke IDEGUCHI[5], Osamu KAMEYA[6], Takahiro KUDOH[7], Yuki KUDOH[8], Mami MACHIDA[9], Yoshimitsu MIYASHITA[10], Hiroshi OHNO[11], Takeaki OZAWA[12], Keitaro TAKAHASHI[10], Motokazu TAKIZAWA[13], and Dai. G. YAMAZAKI[14,12]

Received 12-May-2017; Accepted 05-Sep-2017

Abstract

Magnetic field is ubiquitous in the Universe and it plays essential roles in various astrophysical phenomena, yet its real origin and evolution are poorly known. This article reviews current understanding of magnetic fields in the interstellar medium, the Milky Way Galaxy, external galaxies, active galactic nuclei, clusters of galaxies, and the cosmic web. Particularly, the review concentrates on the achievements that have been provided by centimeter and meter wavelength radio observations. The article also introduces various methods to analyze linear polarization data, including synchrotron radiation, Faraday rotation, depolarization, and Faraday tomography.

Key words: magnetic fields — polarization — radio astronomy

1 Introduction

1.1 Magnetized Universe

Magnetism plays substantial and often essential roles in astronomical objects. Most of known celestial objects, the Earth, planets, the Sun, stars, interstellar space and clouds, the Milky Way Galaxy, galaxies, accretion disks and active galactic nuclei (AGN), and clusters of galaxies are known to be magnetized. An exception might be the Universe where the cosmological isotropy principle has denied the cosmological-scale uniform field, that defines the North and South of the Universe.

The magnetic-field strength, B, is roughly related to the object size, R. Figure 1 depicts the global distribution of magnetic fields in the log B – log R plot. An inverse relation,

* corresponding author: akahori@sci.kagoshima-u.ac.jp; [1]Graduate School of Science and Engineering, Kagoshima University, 1-21-35 Korimoto,

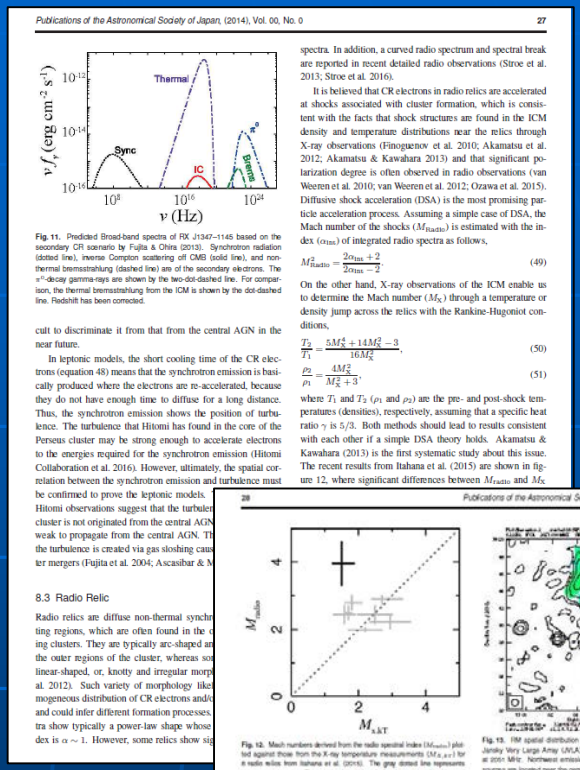

Publications of the Astronomical Society of Japan, (2014), Vol. 00, No. 0 27

Fig. 11. Predicted Broad-band spectra of RX J1347−1145 based on the secondary CR scenario by Fujita & Ohira (2013). Synchrotron radiation (dotted line), inverse Compton scattering off CMB (solid line), and non-thermal bremsstrahlung (dashed line) are of the secondary electrons. The π^0-decay gamma-rays are shown by the two-dot-dashed line. For comparison, the thermal bremsstrahlung from the ICM is shown by the dot-dashed line. Redshift has been corrected.

cult to discriminate it from that from the central AGN in the near future.

In leptonic models, the short cooling time of the CR electrons (equation 48) means that the synchrotron emission is basically produced where the electrons are re-accelerated, because they do not have enough time to diffuse for a long distance. Thus, the synchrotron emission shows the position of turbulence. The turbulence that Hitomi has found in the core of the Perseus cluster may be strong enough to accelerate electrons to the energies required for the synchrotron emission (Hitomi Collaboration et al. 2016). However, ultimately, the spatial correlation between the synchrotron emission and turbulence must be confirmed to prove the leptonic models.

Hitomi observations suggest that the turbulen
cluster is not originated from the central AGN
weak to propagate from the central AGN. Th
the turbulence is created via gas sloshing caus
ter mergers (Fujita et al. 2004; Ascasibar & M

8.3 Radio Relic

Radio relics are diffuse non-thermal synchr
ting regions, which are often found in the
ing clusters. They are typically arc-shaped a
the outer regions of the cluster, whereas so
linear-shaped, or, knotty and irregular morp
al. 2012). Such variety of morphology like
mogeneous distribution of CR electrons and/
and could infer different formation processes.
tra show typically a power-law shape whose
dex is $\alpha \sim 1$. However, some relics show sig

spectra. In addition, a curved radio spectrum and spectral break are reported in recent detailed radio observations (Stroe et al. 2013; Stroe et al. 2016).

It is believed that CR electrons in radio relics are accelerated at shocks associated with cluster formation, which is consistent with the facts that shock structures are found in the ICM density and temperature distributions near the relics through X-ray observations (Finoguenov et al. 2010; Akamatsu et al. 2012; Akamatsu & Kawahara 2013) and that significant polarization degree is often observed in radio observations (van Weeren et al. 2010; van Weeren et al. 2012; Ozawa et al. 2015). Diffusive shock acceleration (DSA) is the most promising particle acceleration process. Assuming a simple case of DSA, the Mach number of the shocks ($M_{\rm Radio}$) is estimated with the index ($\alpha_{\rm ms}$) of integrated radio spectra as follows,

$$M^2_{\rm Radio} = \frac{2\alpha_{\rm ms}+2}{2\alpha_{\rm ms}-2}. \quad (49)$$

On the other hand, X-ray observations of the ICM enable us to determine the Mach number ($M_{\rm X}$) through a temperature or density jump across the relics with the Rankine-Hugoniot conditions,

$$\frac{T_2}{T_1} = \frac{5M_{\rm X}^2+14M_{\rm X}^2-3}{16M_{\rm X}^2}, \quad (50)$$

$$\frac{\rho_2}{\rho_1} = \frac{4M_{\rm X}^2}{M_{\rm X}^2+3}, \quad (51)$$

where T_1 and T_2 (ρ_1 and ρ_2) are the pre- and post-shock temperatures (densities), respectively, assuming that a specific heat ratio γ is 5/3. Both methods should lead to results consistent with each other if a simple DSA theory holds. Akamatsu & Kawahara (2013) is the first systematic study about this issue. The recent results from Itahana et al. (2015) are shown in figure 12, where significant differences between $M_{\rm Radio}$ and $M_{\rm X}$

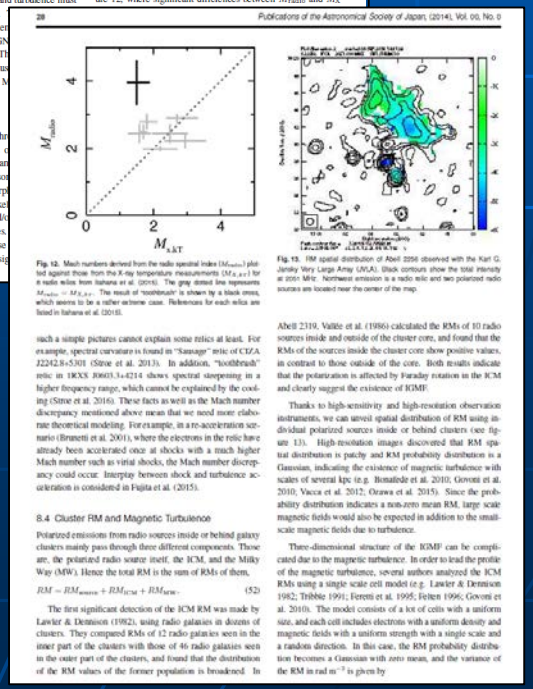

28 Publications of the Astronomical Society of Japan, (2014), Vol. 00, No. 0

Fig. 12. Mach numbers derived from the radio spectral index ($M_{\rm Radio}$) plotted against those from the X-ray temperature measurements ($M_{\rm kT}$) for 8 radio relics from Itahana et al. (2015). The gray dotted line represents $M_{\rm Radio} = M_{\rm kT}$. The result of "toothbrush" is shown by a black cross, which seems to be a rather extreme case. References for each relics are listed in Itahana et al. (2015).

Fig. 13. RM spatial distribution of Abell 2256 observed with the Karl G. Jansky Very Large Array (VLA). Black contours show the total intensity at 20cm MHz. Northwest emission is a radio relic and two polarized radio sources are located near the center of the map.

such a simple pictures cannot explain some relics at least. For example, spectral curvature is found in "Sausage" relic of CIZA J2242.8+5301 (Stroe et al. 2013). In addition, "toothbrush" relic in 1RXS J0603.3+4214 shows spectral steepening in a higher frequency range, which cannot be explained by the cooling (Stroe et al. 2016). These facts as well as the Mach number discrepancy mentioned above mean that we need more elaborate theoretical modeling. For example, in a re-acceleration scenario (Brunetti et al. 2001), where the electrons in the relic have already been accelerated once at shocks with a much higher Mach number such as virial shocks, the Mach number discrepancy could occur. Interplay between shock and turbulence acceleration is considered in Fujita et al. (2015).

8.4 Cluster RM and Magnetic Turbulence

Polarized emissions from radio sources inside or behind galaxy clusters mainly pass through three different components. Those are, the polarized radio source itself, the ICM, and the Milky Way (MW). Hence the total RM is the sum of RMs of them,

$$RM = RM_{\rm source} + RM_{\rm ICM} + RM_{\rm MW}. \quad (52)$$

The first significant detection of the ICM RM was made by Lawler & Dennison (1982), using radio galaxies in dozens of clusters. They compared RMs of 12 radio galaxies seen in the inner part of the clusters with those of 46 radio galaxies seen in the outer part of the clusters, and found that the distribution of the RM values of the former population is broadened. In

Abell 2319, Vallée et al. (1986) calculated the RMs of 10 radio sources inside and outside of the cluster core, and found that the RMs of the sources inside the cluster core show positive values, in contrast to those outside of the core. Both results indicate that the polarization is affected by Faraday rotation in the ICM and clearly suggest the existence of IGMF.

Thanks to high-sensitivity and high-resolution observation instruments, we can unveil spatial distribution of RM using individual polarized sources inside or behind clusters (see figure 13). High-resolution images discovered that RM spatial distribution is patchy and RM probability distribution is a Gaussian, indicating the existence of magnetic turbulence with scales of several kpc (e.g. Bonafede et al. 2010; Govoni et al. 2010; Vacca et al. 2012; Ozawa et al. 2015). Since the probability distribution indicates a non-zero mean RM, large scale magnetic fields would also be expected in addition to the small-scale magnetic fields due to turbulence.

Three-dimensional structure of the IGMF can be complicated due to the magnetic turbulence. In order to lead the profile of the magnetic turbulence, several authors analyzed the ICM RMs using a single scale cell model (e.g. Lawler & Dennison 1982; Tribble 1991; Feretti et al. 1995; Felten 1996; Govoni et al. 2010). The model consists of a lot of cells with a uniform size, and each cell includes electrons with a uniform density and magnetic fields with a uniform strength with a single scale and a random direction. In this case, the RM probability distribution becomes a Gaussian with zero mean, and the variance of the RM in rad m^{-2} is given by

Summary

- Diffuse non-thermal radio emssions are found in some clusters of galaxies (radio halos, relics).
- Radio relics are likely associated with shocks in the ICM.
- Comparison with X-ray and radio observation results provide us with implications of diffusive shock acceleration model.
- Basically, M_X and M_{radio} seems to be consisitent with each other, but some outliers like “toothbrush” may exist.